Acousto-optical nanoscopy of buried photonic nanostructures: supplementary material

T. Czerniuk[1,*], C. Schneider[2], M. Kamp[2], S. Höfling[2], B. A. Glavin[3], D. R. Yakovlev[1,4], A. V. Akimov[5], and M. Bayer[1,4]

[1]Experimentelle Physik 2, Technische Universität Dortmund, 44221 Dortmund, Germany
[2]Technische Physik, Universität Würzburg, 97074 Würzburg, Germany
[3]V. E. Lashkaryov Institute of Semiconductor Physics, 03028 Kyiv, Ukraine
[4]Ioffe Institute, Russian Academy of Sciences, 194021 St. Petersburg, Russia
[5]School of Physics and Astronomy, University of Nottingham, Nottingham NG7 2RD, United Kingdom
[*]Corresponding author: Thomas.Czerniuk@tu-dortmund.de

Compiled April 12, 2017

The supplementary material presented here describes the experimental methods, i.e. the setup and the studied sample, in more detail. In addition, more information about the theoretical model is provided and we discuss to what extent the shape of the acoustic pulse and the photoelastic effect influence the reflectivity modulation.

http://dx.doi.org/10.1364/optica.99.099999.s1 [supplementary document doi]

1. EXPERIMENTAL METHODS

The studied sample was grown by molecular beam epitaxy on a 220 μm thick GaAs substrate. Its two DBRs forming the resonator are made from 33 and 26 periods of alternating AlAs and GaAs quarter wave layers for the bottom and the top mirror, respectively. The thickness of these AlAs and GaAs layers is 74 nm and 69 nm. In between the two mirrors a 266 nm thick λ-cavity spacer made from GaAs is sandwiched. Since the sample has a slight wedge shape, the layer thicknesses vary for different spots on the sample. An ensemble of $Al_{0.09}Ga_{0.55}In_{0.36}As$ quantum dots (QDs) is placed in the cavity layer center and serves as the optically active medium of the laser. Micropillars with different radii ranging from 1.5 μm to 7.5 μm were fabricated in an etching process [1] and studied here. On the backside of the substrate, a 100 nm thick aluminum film was deposited, which is used to create the acoustic pulse like detailed hereafter.

We use the time-resolved pump-probe setup sketched in Fig. S1, where we generate the acoustic pulse with the pump and detect the reflectivity modulation with the probe laser pulse. They are generated by a beam splitter and originate from an amplified laser with a pulse duration of 200 fs, a repetition rate of 100 kHz and a central wavelength of 800 nm. The pump beam is guided over a mechanical delay stage and focused on the backside of the sample to a spot with a FWHM of about 150 μm. In the aluminum film deposited there, the rapid heating following the absorption leads to a thermal expansion, which launches an acoustic pulse into the substrate [2]. The injected displacement profile $u(t)$ can be modeled by a Gaussian. Its FWHM $\theta = v_{Al}/\mu_{Al}$ is given by the optical absorption length μ_{Al} and the sound velocity v_{Al} of aluminum and found to be about 12 ps [3]. For the here applied optical excitation densities of approximately 10 mJ/cm^2, the displacement amplitude is about 50 pm, corresponding to a maximum strain in the order of 10^{-3}. After the injection into the substrate, the pulse propagates with the longitudinal speed of sound towards the micropillar lasers at the sample's front side. Due to the high strain amplitudes, nonlinear propagation must be taken into account and we assume a longer pulse duration of about 90 ps after the substrate transit. On the front surface, a 20 x microscope objective focuses the probe beam to a spot with a diameter of about 15 μm and also collects the reflection, which is guided to a photodiode. To increase the sensitivity for the reflection change originating from the acoustic pulse, we use a lock-in detector together with a mechanical chopper that is placed in the pump beam path. Pump light being scattered from the backside of the sample is not collected by the microscope objective and forwarded into the detection, since the sample is mounted such that it is laterally fully enclosed by a brass mask. The sample is placed in a flow cryostat and attached to a cold finger, whose temperature is kept at 8 K. Due to the laser irradiation and the loose mounting of the sample, which has to ensure access from the front and backside, the local temperature might be elevated.

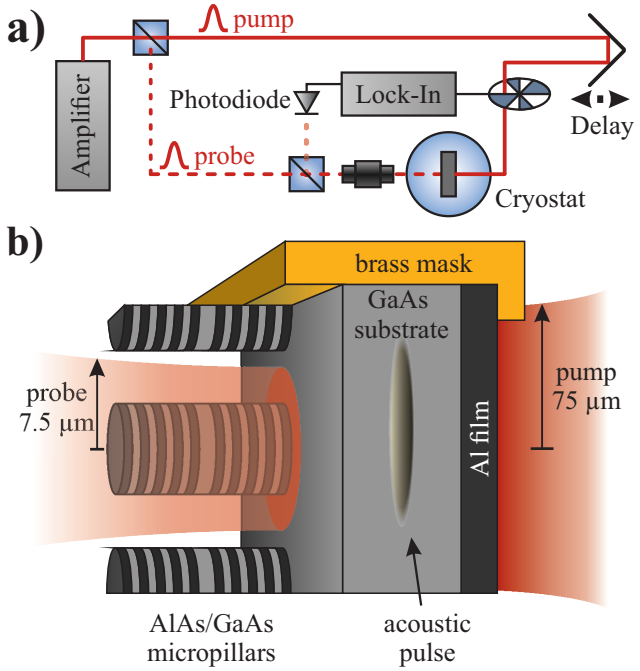

Fig. S1. Experimental methods. Panel (a): Sketch of the experimental setup. Panel (b) Close up of the studied AlAs/GaAs micropillar sample. The probe beam on the front surface detects the acoustic pulse, which is generated by the pump beam in the aluminum film on the sample's backside.

2. VALIDITY OF THE MODEL

This section shall evaluate the simplifications made in the simulations, namely the assumed Gaussian shape of the displacement pulse and the disregard of photoelasticity. For this purpose, we calculate the reflectivity change $\Delta R(t)/R_0$ by a perturbed transfer-matrix with both acousto-optic contributions, i.e. the interface displacement and the photoelastic effect. The shift due to photoelasticity is calculated like in Eq. (1) of the main text with a deformation potential of -7 eV for GaAs and -8 eV for AlAs [4, 5]. The input acoustic pulses are shown in Fig. S2 (a). On the one hand, we choose parabola-shaped displacement profiles with three different FWHM (solid curves). This shape approximates shockwave-like acoustic pulses in the nonlinear regime without their high frequency components like solitons. The duration of the acoustic pulse depends on the initial strain amplitude and the propagation distance. Please note that the amplitude of the low-frequency components saturates for an increasing excitation density, because the spectral weight is shifted more and more towards high-frequency phonons. On the other hand, Gaussians with the same FWHM are employed (dashed curves). The comparison of the reflectivity modulation for these different inputs shall assess the sensitivity of the model to the shape of the acoustic pulse. We consider the same situation like presented in section 3 of the main text, i.e. the same microcavity (with x=0.0) at cryogenic temperatures and the same optical wavelength λ=830 nm. The curves in Fig. S2 (b) show the reflectivity changes induced by the acoustic pulses presented in Fig. S2 (a). The signals due to the parabola-shaped (solid curve) and the Gaussian (dashed curve) displacement pulse look very similar. However, because of the kinks at the front and the tail, the parabola-shaped pulse

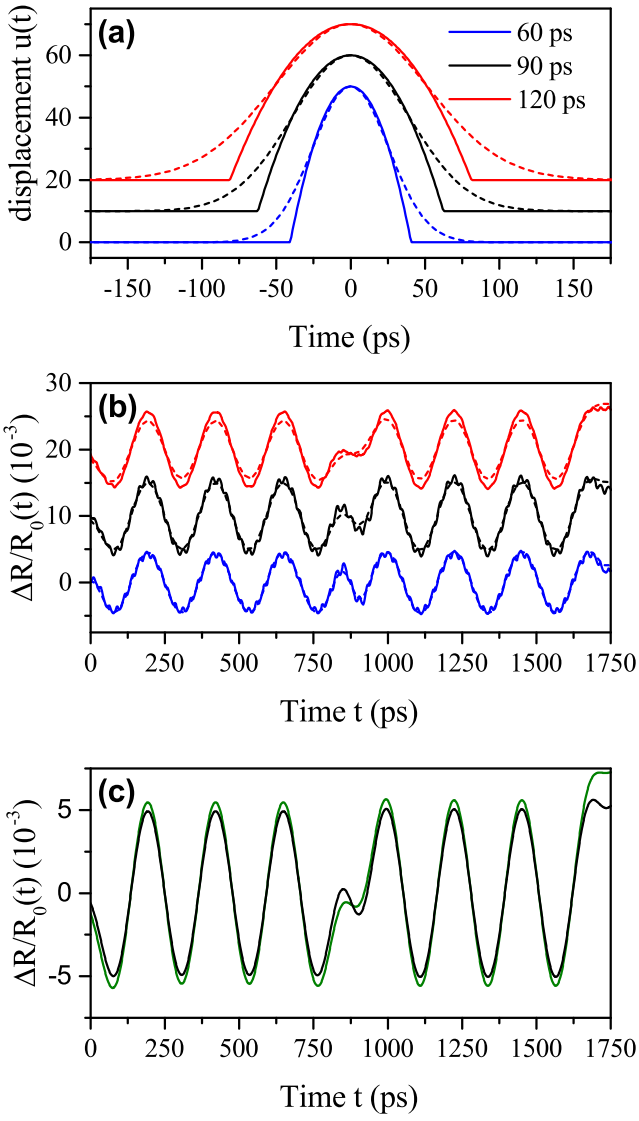

Fig. S2. Validity of the model. Panel (a): Displacement profile $u(t)$ for three different durations of the acoustic pulse. Either a nonlinear-shockwave pulse modeled by a parabola (solid curve) or a Gaussian (dashed curve) is assumed. Panel (b): Simulations for the reflectivity modulation of the modeled planar microcavity (with x=0.0) discussed in the main text due to these acoustic pulses. The simulations include the interface displacement and the photoelastic effect. Panel (c): Reflectivity modulation for the Gaussian with a FWHM of 90 ps with (black curve) and without (green curve) photoelasticity.

contains some remaining high frequency components, which yield additional fast oscillations. In the experiment, the frequencies due to these kinks are filtered by the micropillar. The signal is also independent on the duration of the acoustic pulse. The only notable deviation between the curves with different durations occurs at the transit through the cavity layer at t=0.9 ns. Here, the phase jump of the optical field results in sharp peaks that become more and more smeared out the longer the acoustic pulse lasts. Finally, we discuss the influence of photoelasticity. Fig. S2 (c) shows the full simulations with (black curve) and without (green curve) the photoelastic effect for the Gaussian with a FWHM of 90 ps. One can see that the displacement effect dominates the total response. In the present case, this is achieved by choosing a wavelength for which the materials are (i) transparent and (ii) the derivative of the dispersion is minimum.

REFERENCES

1. S. Reitzenstein and A. Forchel, "Quantum dot micropillars," J. Phys. D: Appl. Phys. **43**, 033001 (2010).
2. C. Thomsen, J. Strait, Z. Vardeny, H. J. Maris, J. Tauc, and J. J. Hauser, "Coherent phonon generation and detection by picosecond light pulses," Phys. Rev. Lett. **53**, 989 (1984).
3. A. D. Rakić, A. B. Djurišić, J. M. Elazar, and M. L. Majewski, "Optical properties of metallic films for vertical-cavity optoelectronic devices," Appl. Opt. **37**, 5271 (1998).
4. F. H. Pollak and M. Cardona, "Piezo-Electroreflectance in Ge, GaAs, and Si," Phys. Rev. **172**, 816 (1968).
5. O. Madelung, U. Rössler, and M. Schulz, eds., *Aluminum arsenide (AlAs), band structure parameters, deformation potentials* (Springer Berlin Heidelberg, 2002).